Collisional Breakup in Coulomb Systems

T.N. Rescigno[1,2] and C.W. McCurdy[1,3]

[1]Lawrence Berkeley National Laboratory
Computing Sciences
Berkeley, CA 94720, USA
[2]Lawrence Livermore National Laboratory
Physics and Advanced Technologies
Livermore, CA 94551, USA
[3]University of California, Davis
Department of Applied Science
Davis, CA 95616, USA

1 Introduction

Atomic collision theorists have struggled to understand the details of the simplest problem in collisional ionization - the electron-impact ionization of atomic hydrogen - since the formulation of the problem some forty years ago by Peterkop [1] and by Rudge and Seaton [2]. In fact, it is only within the last few years that this problem has been reduced to "practical computation", meaning one has a formalism and the associated numerical algorithms that permit the calculation, with currently available computing capability, of the relevant physical quantities to any accuracy that can be tested by experiment. That fact has been demonstrated, for example, in a series of papers [3–8] applying the ideas of exterior complex scaling of electronic coordinates to the electron-impact ionization of the hydrogen atom. Other methods including convergent close-coupling[9–11], the R-matrix pseudostates method[12], hyperspherical close-coupling[13,14], and time-dependent close-coupling[15] have also been applied to aspects of this problem with great success. For the related problem of double-photoionization of helium, the hyperspherical R-matrix method[16] has used with great success.

The central difficulty that impeded progress on the problem of three-body breakup in Coulomb systems, particularly for the collisional breakup or "e,2e" problem (as opposed to double photoionization), is the cumbersome asymptotic form of the scattering wave function that the formal theory of ionization imposes. The appropriate boundary condition for ionization, deduced by Peterkop [1] and Rudge and Seaton [2], is

$$\Psi^{+}_{\rm ion}(\mathbf{r}_1,\mathbf{r}_2) \underset{\rho\to\infty}{\longrightarrow} -f_i(\hat{r}_1,\hat{r}_2,\alpha)\sqrt{\tfrac{i\kappa^3}{\rho^5}}\exp\{i[\kappa\rho+\frac{\zeta(\hat{r}_1,\hat{r}_2,\alpha)}{\kappa}\ln(2\kappa\rho)]\}, \tag{1}$$

where f_i is the ionization amplitude and the hyperspherical coordinates are defined by $\rho=(r_1^2+r_2^2)^{1/2}$ with $\alpha=\tan^{-1}(r_1/r_2)$, and κ is related to the total

energy by $E = \kappa^2/2$. The most obvious difficulty in applying this boundary condition is that the coefficient $\zeta(\hat{r}_1, \hat{r}_2, \alpha)$ of the logarithmic phase depends on the distances and ejection angles of both electrons. However, worse yet is the fact that Eq. (1) is not separable in spherical coordinates, and is therefore much more cumbersome to apply to numerical calculations which are perforce done in that coordinate system. As a consequence, no one has yet applied Eq.(1) to the numerical solution of the Schrödinger equation for the ionization problem.

The formal theory of ionization poses another challenge to computation as well, and that is that the ordinary expression for evaluating the amplitude, starting from the scattering wave function that solves the Schrödinger equation, does not apply, because defined in the usual way it would have an infinite phase associated with integrating an expression with logarithmic phases over an infinite volume. Instead the amplitude is given by [1,2,17]

$$f(\mathbf{k}_1, \mathbf{k}_2) = -(2\pi)^{5/2} e^{i\Delta(\mathbf{k}_1, \mathbf{k}_2)} \iint \Psi^+ (H - E)\phi(-\mathbf{k}_1, z_1)\phi(-\mathbf{k}_2, z_2) d\mathbf{r}_1 d\mathbf{r}_2 \tag{2}$$

with *effective charges* in the one-body Coulomb functions, $\phi(-\mathbf{k}, z)$ depending on both the energy and direction of ejection of each electron,

$$\frac{z_1}{k_1} + \frac{z_2}{k_2} = \frac{1}{k_1} + \frac{1}{k_2} - \frac{1}{|\mathbf{k}_1 - \mathbf{k}_2|}, \tag{3}$$

and with

$$\Delta(\mathbf{k}_1, \mathbf{k}_2) = 2[(z_1/k_1)\ln(k_1/\kappa) + (z_2/k_2)\ln(k_2/\kappa)]. \tag{4}$$

Both of these difficulties were ultimately overcome by the successful methods for treating the electron-impact ionization problem. The first of them, the asymptotic form in Eq.(1), was the central issue addressed by the Exterior Complex Scaling (ECS) method, which is the principal subject of this chapter. The second of them, the Coulomb breakup amplitude formula in Eq.(2) and its attendant numerical pathologies, required a reformulation and the observation that numerical computations on a finite volume can be at most affected by a finite overall phase that leaves physical observables unchanged.

2 Exterior Complex Scaling - Circumventing Asymptotic Boundary Conditions

The ECS method owes its origins to the long history of complex scaling methods in atomic and molecular physics, which in turn is based on a very simple observation about the behavior of solutions of the Schrödinger equation when viewed as functions of complex variables. A purely outgoing wave, $\exp(ikr)$, with $k > 0$, becomes exponentially decaying when the coordinate, r, is scaled

into the upper half complex plane, $\exp(ikre^{i\eta}) \to 0$ as $r \to \infty$. The first step in the ECS formalism, therefore, is to isolate the outgoing or "scattered wave" portion of the full scattering wave function. To that end, we partition the full wave function into an initial unperturbed state, Φ_0, and a scattered wave, Ψ_{sc}, which contains only outgoing waves in all channels:

$$\Psi^{(+)} = \Psi_{sc} + \Phi_0. \tag{5}$$

For a two-electron, problem, e.g., electron-hydrogen atom scattering, Φ_0 can be written, for singlet (upper sign) or triplet (lower sign) spin coupling,

$$\Phi_0 = \frac{1}{\sqrt{2k_0}}(e^{i\mathbf{k_0}\cdot\mathbf{r_1}}\varphi_0(\mathbf{r_2}) \pm \mathbf{e}^{\mathbf{ik_0}\cdot\mathbf{r_2}}\varphi_\mathbf{0}(\mathbf{r_1})), \tag{6}$$

where $\mathbf{k_0}$ is the incident electron momentum, and φ_0 is the initial state of the atom. The scattered wave then satisfies the driven Schrödinger equation for a particular initial condition,

$$(E - H)\Psi_{sc} = (H - E)\Phi_0. \tag{7}$$

Complex scaling reduces the Coulomb boundary condition for breakup, with its complicated logarithmic phases, to the trivial condition that $\Psi_{sc}(\mathbf{r}_1, \mathbf{r}_2)$ vanish at infinity. The subtlety in the (e,2e) problem is that we must extract the physics of breakup from Ψ_{sc} in a region in which the coordinates on which it depends are real, so we need to apply the complex scaling transformation only when either of the coordinates of the two electrons are greater than some radius, R_0. The ECS transformation that does this was invented and investigated in the context of electron scattering resonances with only one electron in the continuum [18,19]; its adaptation to the (e,2e) problem is shown in Fig.(1). Specifically, under ECS, the radial coordinates of the electrons are transformed under the mapping:

$$r \to \begin{cases} r & r < R_0, \\ R_0 + (r - R_0)e^{i\eta} & r \geq R_0. \end{cases} \tag{8}$$

Because Ψ_{sc} contains only outgoing waves, which decay exponentially on the complex part of the exterior scaling contour, Eq.(7) can be solved by applying only the boundary condition that Ψ_{sc} vanish at large distances. On the real part of the contour, Ψ_{sc} is the correct physical wave function from which all scattering information can, in principle, be extracted, provided it is extracted in the region of real coordinates.

There is one final subtlety: because Eq.(6) contains plane waves, which diverge under complex scaling, interaction potentials must be truncated at large distances, but only on the right hand side of Eq.(7) [20].

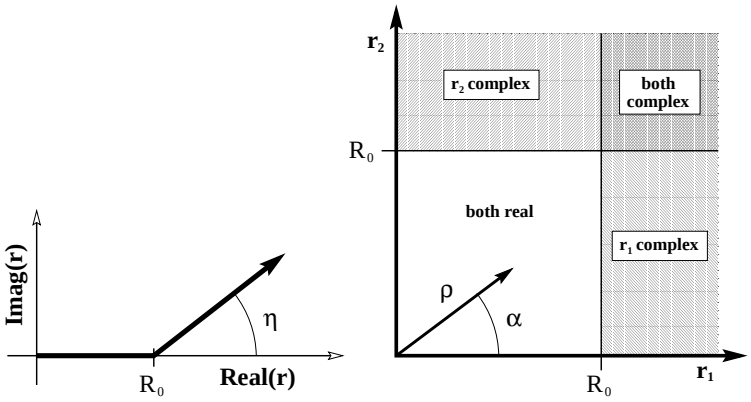

Fig. 1. Left Panel: illustration of the ECS contour rotated into the upper-half of the complex r-plane beyond R_0. Right Panel: Depiction of exterior complex scaling for two radial coordinates.

3 Scattered-Wave Formalism - Options for Computing the Wave Function

The method of exterior complex scaling and its applications have been developed in a series of papers [3–8,21–23], which from the outset divided the solution of the problem of electron-impact ionization into two discrete steps:

1. Compute the scattering wave function without recourse to the explicit three-body asymptotic form by applying exterior complex scaling to the solution of a discretized representation of the Schrödinger equation.
2. Extract differential and total ionization cross sections from the wave function by either "interrogating" it to compute the scattered flux, or using it in an integral expression for the breakup amplitudes.

It is worth noting that these two problems, namely the computation of the scattered wave function and the subsequent extraction of the scattering information, are only distinct steps in approaches where the wave function is computed by a method that is independent of the asymptotic matching condition that defines the scattering amplitudes. In that sense, our approach is similar to time-dependent methods which track a wavepacket through the collision from initial to final states and then attempt to extract cross sections by analyzing the exiting wavepacket. It is also the case with both approaches that the extraction step, while far from being the most computationally intensive part of the overall calculation, presents many formal difficulties, particularly in the case on multi-electron targets, and is the subject of much current research.

3.1 Time-Independent Approach - Linear Equations

To solve the scattered wave Schrödinger equation, Eq. (7), we must specify the underlying representation. For all the ECS calculations to date, Ψ_{sc} is first expanded in coupled spherical harmonics of the angular coordinates of the two electrons: $\mathcal{Y}^{L0}_{l_1,l_2}(\hat{\mathbf{r}}_1,\hat{\mathbf{r}}_2)$

$$\Psi_{sc}(\mathbf{r}_1,\mathbf{r}_2) = \sum_{L,l_1,l_2} \Psi^L_{l_1,l_2}(r_1,r_2)\mathcal{Y}^{L0}_{l_1,l_2}(\hat{\mathbf{r}}_1,\hat{\mathbf{r}}_2) \tag{9}$$

thereby allowing the conversion of Eq.(7), the driven Schrödinger equation, to a set of coupled equations for the two-particle radial functions, $\Psi^L_{l_1,l_2}(r_1,r_2)$:

$$\begin{aligned}&\left(E - \hat{H}_{l_1}(r_1) - \hat{H}_{l_2}(r_2)\right)\psi^L_{l_1l_2}(r_1,r_2)\\ &\quad - \sum_{l_1',l_2'}\langle l_1l_2||l_1'l_2'\rangle_L \psi^L_{l_1',l_2'}(r_1,r_2) = \chi^L_{l_1l_2}(r_1,r_2)\end{aligned} \tag{10}$$

where the radial coupling potentials, $\langle l_1l_2||l_1'l_2'\rangle_L$, are obtained by taking matrix elements of $\frac{1}{|\mathbf{r}_1-\mathbf{r}_2|}$ between two coupled spherical harmonics [6]. The inhomogeneous terms, $\chi^L_{l_1l_2}$, arise from the partial-wave expansion of the right-hand side of Eq.(7)

The set of coupled equations is converted to a system of linear equations by choosing some discretization method for representing the exterior-scaled radial functions. In our earlier studies of e-H ionization, the coupled radial equations were solved on a complex two-dimensional grid using seven-point finite difference approximations to the second derivatives. A typical calculation might have ~ 450 points in each radial dimension, and for a given total angular momentum, L, have of the order of 24 (l_1,l_2) angular momentum pairs. The time consuming step of the calculation, now a modest computation on a massively parallel supercomputer, is the solution of sparse linear equations of the order of five million. To accomplish this, we used an iterative algorithm specifically tailored to the problem at hand. The eigenvalue spectrum of a complex-scaled Hamiltonian is such that no known iterative algorithm will converge to solution without pre-conditioning. Therefore, finding a suitable pre-conditioner for the coupled equations is a necessity. The set of *uncoupled* radial equations, defined by setting $\langle l_1l_2||l_1'l_2'\rangle_L = 0$ for all $(l_1',l_2') \neq (l_1,l_2)$ in Eq. (10), have numerical properties similar to the coupled equations, but require solving linear systems only as big as the total number of radial grid points. We have found solutions of the uncoupled equations, which can be obtained by using a direct sparse solver [24], to be a suitable pre-conditioner for solving the coupled equations.

The coupled equations can be solved using discretization schemes that are more efficient that high-order finite difference. In our current efforts, we use a combined finite element and discrete variable representation (DVR), which is the most efficient numerical representation developed to date[25].

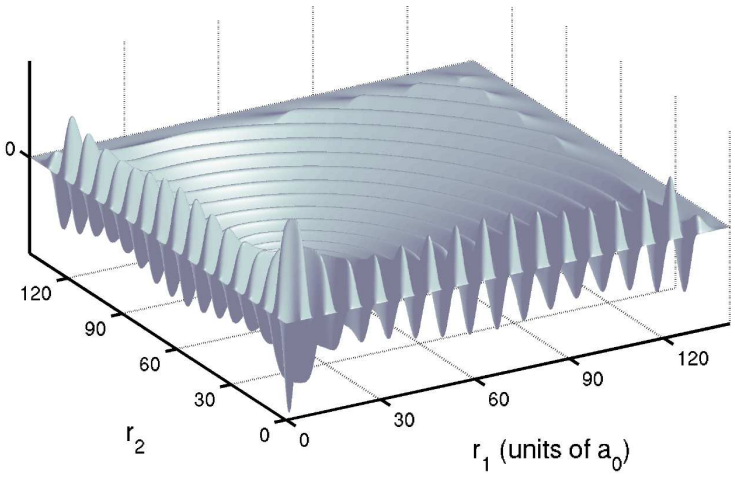

Fig. 2. Real part of a representative radial function for electron-hydrogen scattering at 17.6 eV incident energy. Vertical axis is $Re(\Psi)$ and the two horizontal axes are r_1 and r_2 with origins at the rear left corner. $\Psi^L_{l_1,l_2}(r_1,r_2)$ is shown for singlet spin, $L=2$ and $l_1=l_2=1$

In that representation a DVR using Lobatto shape functions is constructed inside each finite element. Continuity of the wave function is enforced at the boundaries of the finite elements, and one of those boundaries is always chosen to lie at R_0. The finite-element DVR representation of the one-dimensional kinetic energy, $-\frac{1}{2}\partial^2/\partial r^2$, has a blocked structure, but the potentials, both $v(r)$ and $V(r_i,r_j)$, are diagonal in the coordinates of each electron. Since the underlying grid points are connected to a Gauss quadrature rule, the total number of points required is considerably smaller than what would be required with finite difference to achieve the same level of accuracy.

For the e-H problem, one of the many calculated radial functions contributing to Ψ_{sc} is shown in Fig.(2). In that figure one can see the outgoing flux in the discrete, inelastic channels going out near the axes, while the ionization flux goes out for large r_1 and r_2 in the structures resembling ripples from a pebble dropped in a pond.

3.2 Time-Dependent Approach - Wavepacket Propagation

A straightforwad extension of the method outlined in the previous section to a two-electron target atom, for example to the case of e-He ionization, would require the solution of coupled linear equations in three radial dimensions. The most troublesome aspect of such an undertaking, aside from the computer resources that would be required, is the fact that even the *uncoupled* equations would likely require an iterative method of solution and finding a suitable

pre-conditioner would be difficult. In contrast to time-independent methods, explicit time-dependent methods, which involve propagating a wavepacket on a multi-dimensional grid, have scaling properties that allow their application to three-electron systems. We have recently described a step toward a complete algorithm for solving the three-electron breakup problem by combining the idea of time propagation with that of using exterior complex scaling to solve a driven Schrödinger equation [26].

Exterior complex scaling had previously been explored as a method for solving the time-dependent Schrödinger equation [27,28]. The critical observation in that work is that if the wave packet $\Psi(\mathbf{r};t)$ contains only outgoing waves, then

$$\Psi(R(\mathbf{r});t) \xrightarrow[r\to\infty]{} 0 \tag{11}$$

on the complex contour for all times, t. Since the physical solution of the driven Schrödinger equation in Eq.(7) has only outgoing waves, that point is the key to the time-dependent formulation of the ECS method for the present problem.

Formally, the solution of Eq.(7) we seek is

$$\Psi_{sc}(\mathbf{r}_1,\mathbf{r}_2,\dots) = G^{(+)}(H-E)\Phi_0(\mathbf{r}_1,\mathbf{r}_2,\dots), \tag{12}$$

with $G^{(+)}$ being the Green's function with outgoing wave boundary conditions,

$$G^{(+)} = (E - H + i\epsilon)^{-1}. \tag{13}$$

We can also write $G^{(+)}$ formally as

$$G^{(+)} = \frac{1}{i}\int_0^\infty e^{i(E+i\epsilon)t}e^{-iHt}dt. \tag{14}$$

Note that the r.h.s. of Eq.(7) satisfies

$$(H-E)\Phi_0(\mathbf{r}_1,\mathbf{r}_2,\dots) \xrightarrow[r_i\to\infty]{} 0 \tag{15}$$

because Φ_0 is asymptotically an eigenfunction of H. In fact $(H-E)\Phi_0$ has the range of the interaction potential. In general, therefore, we can define a square-integrable wave packet, $\chi(\mathbf{r}_1,\mathbf{r}_2,\dots;t)$, by

$$\chi(\mathbf{r}_1,\mathbf{r}_2,\dots;t) = e^{-iHt}(H-E)\Phi_0(\mathbf{r}_1,\mathbf{r}_2,\dots). \tag{16}$$

Now if we apply the exterior scaling transformation to this equation and define the exterior scaled Hamiltonian by,

$$H \to H_{ECS} = H(R(\mathbf{r}_1),R(\mathbf{r}_2),\dots), \tag{17}$$

where the scaling applies only to the radial coordinates, the wave packet then becomes

$$\chi(R(\mathbf{r}_1), R(\mathbf{r}_2), \dots ; t) = e^{-iH_{ECS}t}(H_{ECS} - E) \times \Phi_0(R(\mathbf{r}_1), R(\mathbf{r}_2), \dots). \tag{18}$$

This packet has two important properties,

$$\chi(R(\mathbf{r}_1), R(\mathbf{r}_2), \dots ; t) \xrightarrow[r_i \to \infty]{} 0, \tag{19}$$

and

$$\chi(R(\mathbf{r}_1), R(\mathbf{r}_2), \dots ; t) \xrightarrow[t \to \infty]{} 0, \tag{20}$$

Therefore we can write Ψ_{sc} simply as the Fourier transform of the the wave packet

$$\Psi_{sc} = \frac{1}{i} \int_0^\infty e^{iEt} \chi(t) dt, \tag{21}$$

and the $+i\epsilon$ in Eq.(14) is unnecessary.

Eq.(21) provides a numerical representation of Ψ_{sc}, provided we can propagate $\chi(0) = (H - E)\Phi_0$ on the ECS contour in two or three dimensions. In numerical experiments we have found that the class of numerical propagators that are unitary for hermitian Hamiltonians, i.e., before the ECS transformation is made, are generally stable for the corresponding exterior scaled Hamiltonians. For example in one dimension it has been shown[28] that the Cranck-Nicolson propagator, for time step Δt,

$$e^{-iH\Delta t} = (1 + iH\Delta t/2)^{-1}(1 - iH\Delta t/2) + \mathcal{O}((\Delta t)^3). \tag{22}$$

works well as does the two-dimensional version of this propagator.

The motivation behind the time-dependent approach is the development of a method that scales favorably with particle number, so it should not involve solutions of linear equations representing multiple dimensions at each time step. In our current work, we are using a simple version of the split operator approach [29], in which we first write,

$$H = \sum_{i=1}^{d} H_0(r_i) + \sum_{i>j=1}^{d} V(r_i, r_j), \tag{23}$$

where $H_0(r)$ is the one-body Hamiltonian and $V(r_i, r_j)$ is the two-body interaction potential, and then approximate the propagator by,

$$e^{-iH\Delta t} \approx e^{-i\sum_{i>j} V(r_i,r_j)\Delta t/2} \left[\prod_{i=1}^{d} e^{-iH_0(r_i)\Delta t}\right] e^{-i\sum_{i>j} V(r_i,r_j)\Delta t/2}. \tag{24}$$

With either finite-difference or DVR, the potentials are diagonal in the coordinates of each electron. The operators $\exp(-iH_0(r_i)\Delta t)$ can be represented by an $N \times N$ matrix, where N is the number of grid points in one dimension, that need be computed only once. It is straightforward to show [26] that, for a problem with d dimensions, the entire propagator requires $\mathcal{O}(2N^d) + \mathcal{O}(dN^{d+1})$ operations per time step. The scaling advantage of the time-dependent approach as outlined above is then that of N^{d+1} versus N^{2d} for the time-independent approach.

4 Extraction of Physical Cross Sections

With the scattering wave function in hand we are faced with the problem of extracting the information it contains about elastic, discrete inelastic and ionization channels. A complete theoretical treatment of electron-impact ionization must necessarily include a prescription for calculating differential cross sections that give detailed information about the energies and angles of ejection of both electrons. Unlike the representation of the wave function in an ordinary atomic close-coupling calculation, its numerical representation in this approach gives no immediate indication of how to separate those contributions.

4.1 Flux-Operator Approach

The first ECS calculations on electron-impact ionization of hydrogen were performed by simply computing a variant of the quantum mechanical flux through a surface that lies within the volume of coordinate space where both coordinates are real. The continuum of ionization final states is described by flux through a hypersphere of radius ρ_0 in the limit $\rho_0 \to \infty$. To this end, we define a generalized, dimensionless flux $\mathsf{f}_{\rho_0}^{(\mathrm{ion})}$

$$\begin{aligned}\mathsf{f}_{\rho_0}^{(\mathrm{ion})}(\alpha, \hat{r}_1, \hat{r}_2) \equiv\ & \mathrm{Im}\Big[k_i \rho \left(r_1 r_2 \Psi_{\mathrm{ion}}^{+}(\mathbf{r}_1, \mathbf{r}_2)\right)^{\star} \times \\ & \frac{d}{d\rho}\left(r_1 r_2 \Psi_{\mathrm{ion}}^{+}(\mathbf{r}_1, \mathbf{r}_2)\right)\Big]\Big|_{\rho=\rho_0}\end{aligned} \tag{25}$$

evaluated at a hyperradius ρ_0. Since the hyperspherical angle α parametrizes the momentum distribution between the two electrons as $\rho_0 \to \infty$, we can express the total ionization cross section as an integral of $\mathsf{f}_{\rho_0}^{(\mathrm{ion})}$, in the limit $\rho_0 \to \infty$, over α and the angular coordinates of both electrons:

$$\sigma_{\mathrm{ion}} = \frac{1}{k_i^2} \int_0^{\pi/2} \int_{4\pi} \int_{4\pi} \mathsf{f}_{\rho_0}^{(\mathrm{ion})}(\alpha, \hat{r}_1, \hat{r}_2)\ d\hat{r}_1 d\hat{r}_2 d\alpha \Bigg|_{\rho_0 \to \infty} \tag{26}$$

Thus, the $\rho_0 \to \infty$ limit of the flux leads directly to a differential cross section for ionization. To compute the scattered flux, we assemble $\Psi^+_{\rm sc}$ and $\frac{d}{d\rho}\Psi^+_{\rm sc}$ from all its partial wave components:

$$\mathsf{f}_{\rho_0}(\alpha,\hat{r}_1,\hat{r}_2) = \\ \mathrm{i}\left\{ k_i\rho \sum_{\substack{L',l'_1,l'_2 \\ L,l_1,l_2}} \left(\psi^{L'}_{l'_1 l'_2}\right)^\star \frac{d}{d\rho}\left(\psi^{L}_{l_1 l_2}\right) \left(\mathcal{Y}^{L'0}_{l'_1,l'_2}(\hat{\mathbf{r}}_1,\hat{\mathbf{r}}_2)\right)^\star \mathcal{Y}^{L0}_{l_1,l_2}(\hat{\mathbf{r}}_1,\hat{\mathbf{r}}_2) \right\}\Bigg|_{\rho=\rho_0} \tag{27}$$

The flux operator approach, while conceptually straightforward, is computationally difficult. For purely geometrical reasons, the calculation of the asymptotic flux can require calculations well beyond the range of the potentials, even in the case of short-ranged interactions. Indeed, by inserting the asymptotic form for $\Psi^+_{\rm ion}$ from Eq. (1) into Eq. (25) we find that the ionization flux approaches its asymptotic limit as $\frac{1}{\rho}$, *i.e.* for large ρ_0

$$\mathsf{f}^{(\rm ion)}_{\rho}(\alpha,\hat{r}_1,\hat{r}_2) \;=\; \mathsf{f}^{(\rm ion)}_{\infty}(\alpha,\hat{r}_1,\hat{r}_2) + \mathcal{O}\left(\frac{1}{\rho_0}\right) \tag{28}$$

The calculated flux must therefore be numerically extrapolated to infinite ρ_0 to obtain physical results.

A more serious problem, evident in the plot of the radial wave function shown in Fig. (2), is that there are regions of space (near the axes) where the "ionization wave" overlaps the discrete two-body channels. The fact that the latter contaminate the ionization flux again forces one to employ grids large enough to allow the physical region inhabited only by the ionization portion of the scattered wave to be distinguishable from the parts that describe discrete two-body channels. The angular range in α subtended by the flux due to a discrete channel is $sin^{-1}(\Delta/\rho_0)$ where Δ is the distance over which the target state is appreciably different from zero. Thus as ρ_0 increases, contamination of the ionization flux from discrete channels is confined to smaller regions of α. In the true $\rho_0 \to \infty$ limit the discrete channels' contributions to the flux become delta functions at $\alpha = 0$ and $\alpha = 90^o$ and equality in Eq. (28) holds except for infinitesimally small regions near the edges. In practice, the contamination of the ionization flux by discrete channels on finite grids limits the flux-extrapolation procedure in its ability to describe ionization when a single electron carries most of the available energy. Our early calculations of singly differential cross sections(SDCS) [5] were limited to cases where one electron carried no more than about 75% of the total energy.

The most detailed information about ionization is contained in the so-called triply differential cross section(TDCS) which measures the energy and angles of the two outgoing electrons. The calculated TDCS for electron-hydrogen ionization at 17.6eV incident energy is compared with the absolute experimental measurements of Röder *et al.* [30] in Fig.(3). The results are shown for the coplanar symmetric experimental geometry (which means that

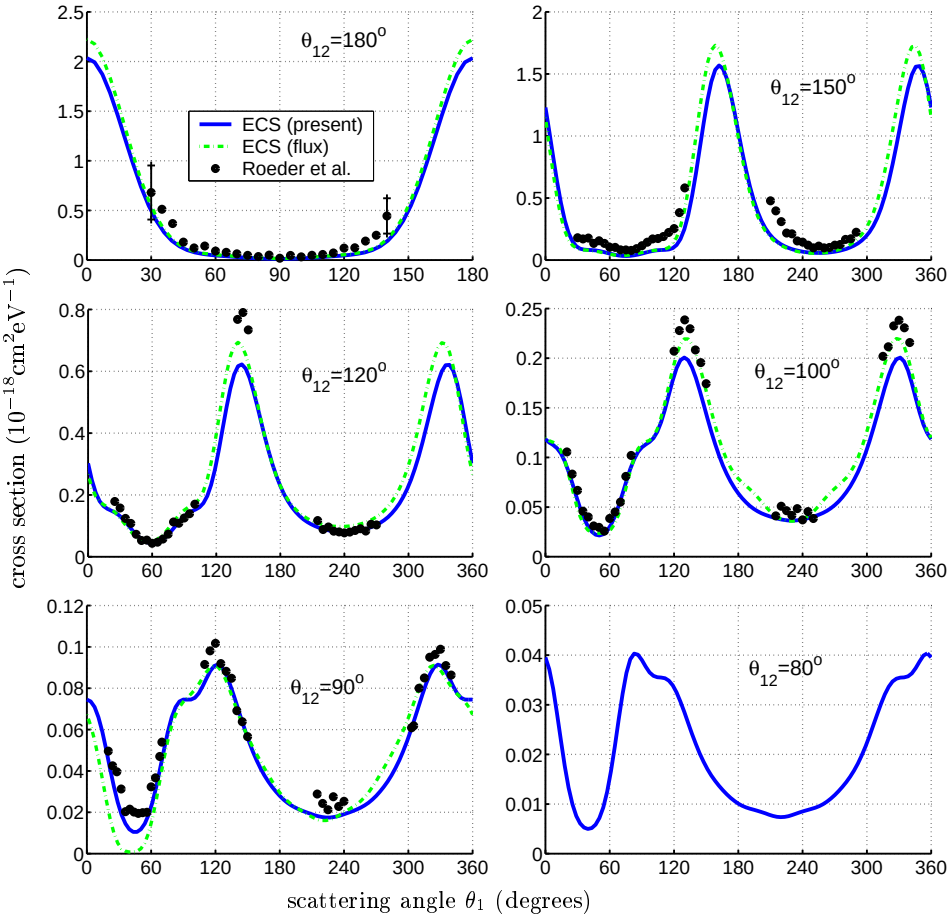

Fig. 3. Equal-energy sharing, coplanar TDCS for electron-hydrogen ionization at 17.6 eV incident energy shown for geometries with θ_{12} fixed. Experimental data are absolute measurements of Röder *et al* with 40% error bars. Dark solid curves: integral expression for breakup amplitude, Lighter curves: flux extrapolation.

the incident electron and both exiting electrons lie in a plane, *and* the two exiting electrons have equal energy), with a fixed angle between the exiting electrons. There has been some question about about the internormalization of these measurements with others done by holding the direction of one exiting electron fixed, but previously unpublished results in J. Röder's thesis have recently resolved that discrepancy [31]. From 19.6 eV to 30eV only relative measurements are available, but excellent agreement with them is attained in ECS calculations, as is demonstrated in Fig.(4).

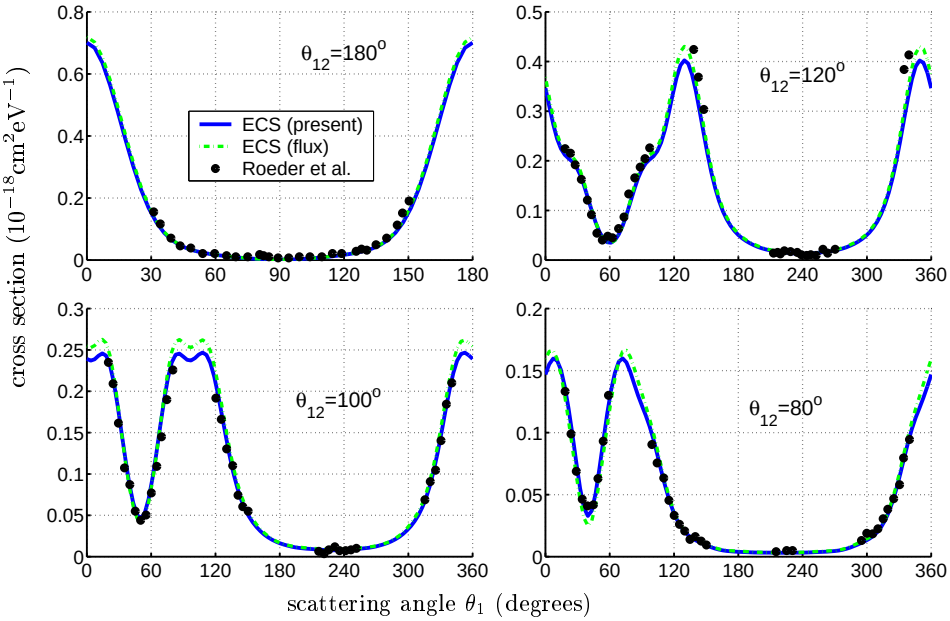

Fig. 4. TDCS for 25 eV incident energy. Normalization factor to convert measured values of Röder *et al.* from arbitrary units is 0.16.

4.2 Formal Rearrangement Theory and Scattering Amplitudes for Three-Body Breakup

While the straightforward evaluation of quantum mechanical flux has the appeal that it corresponds to the most basic formal definition of the cross sections, it is not as efficient, even for simple inelastic scattering, as the calculation of scattering amplitudes via matrix elements that depend only on the range of the interaction potential. It is therefore advantageous, both computationally and theoretically, to confront the dilema posed by the formal theory in Eqs.(2-4).

The question of how to formulate a procedure for extracting breakup amplitudes from a wave function that is only known numerically on a finite grid was addressed in a series of recent papers [8,22,23]. In the first of these studies [22] we showed that, even in cases that involve only short-ranged potentials, some formally correct integral expressions for the breakup amplitudes can yield numerically unstable or poorly convergent results. For example, the expression

$$f = \langle \mathbf{p_1}, \mathbf{p_2} | \mathbf{V} | \Psi^+ \rangle \tag{29}$$

where the final state is just a product of plane waves, while providing a formally correct breakup amplitude for short-ranged potentials, was found to be

numerically unstable. The instability can be traced to 'free-free' overlap terms that arise from discrete two-body channels in the scattered wave function. On an infinite grid, these terms are proportional to momentum conserving delta functions which therefore contribute nothing to the breakup amplitude, but on a finite grid, they are a source of numerical error. A practical solution was found by using formal rearrangement to express the amplitude in terms of distorted waves. A series of formal manipulations, combined with Green's theorem, allows us to express the breakup amplitude as a surface integral:

$$f = \frac{1}{2}\int_S (\phi^{(+)}_{k_1}\phi^{(+)}_{k_2}\nabla\Psi^+_{\rm sc} - \Psi^+_{\rm sc}\nabla\phi^{(+)}_{k_1}\phi^{(+)}_{k_2})\cdot d\hat{\mathbf{S}} \tag{30}$$

where the functions $\phi^{(+)}_k$ are distorted waves derived from the one-body terms in the interaction potential [22].

For Coulomb problems, the obvious extension is to employ Coulomb functions as distorted waves in Eq. (30). This is, however, at odds with the formal theory, which states that the integral expression in Eq. (30) will have a divergent phase unless the Coulomb functions are chosen with effective charges that satisfy Eq. (3). But the use of effective charges other than unity in the Coulomb functions that define the final state have the unfortunate property of destroying their orthogonality to the bound states of the hydrogen atom. We showed in ref. [23] that, on a finite volume, the effect of using Coulomb functions with $Z = 1$ in computing the ionization amplitudes is merely to introduce an inconsequential overall phase that has no effect on the cross section. It is the application of the integral formula, together with the ECS method, to ionization of hydrogen that has given the most accurate description of the complete dynamics to date [8] and which does in fact "reduce the problem to practical computation". The TDCS results obtained from the integral amplitudes, which are also shown in Figs. (3) and (4), attest to the accaracy of approach and also validate the fundamental correctness of the earlier flux extrapolation approach.

The magnitudes and shapes of the singly differential cross sections at low energies give a particularly compelling demonstration of the ECS approach and make a satisfying connection with the semiclassical theories that have been applied to the threshold behavior of the ionization process. Fig.(5) compares the SDCS computed by flux extrapolation and from integral amplitudes at incident energies from 15.4 eV (only 2 eV above the ionization threshold) to 54.4 eV. At lower energies the flux and integral formula methods for computing the SDCS disagree by as much as 10%, because the extrapolation of the flux becomes increasingly difficult as the energy is lowered. However no such difficulty affects the integral expression in Eq.(30). At very low energies the SDCS is almost flat and almost constant as a function of incident energy. If it were flat and constant it would correspond to a linear threshold law for the total cross section. In semiclassical calculations at the Wannier geometry with electrons exiting in opposite directions, Rost [32] predicted qualitatively

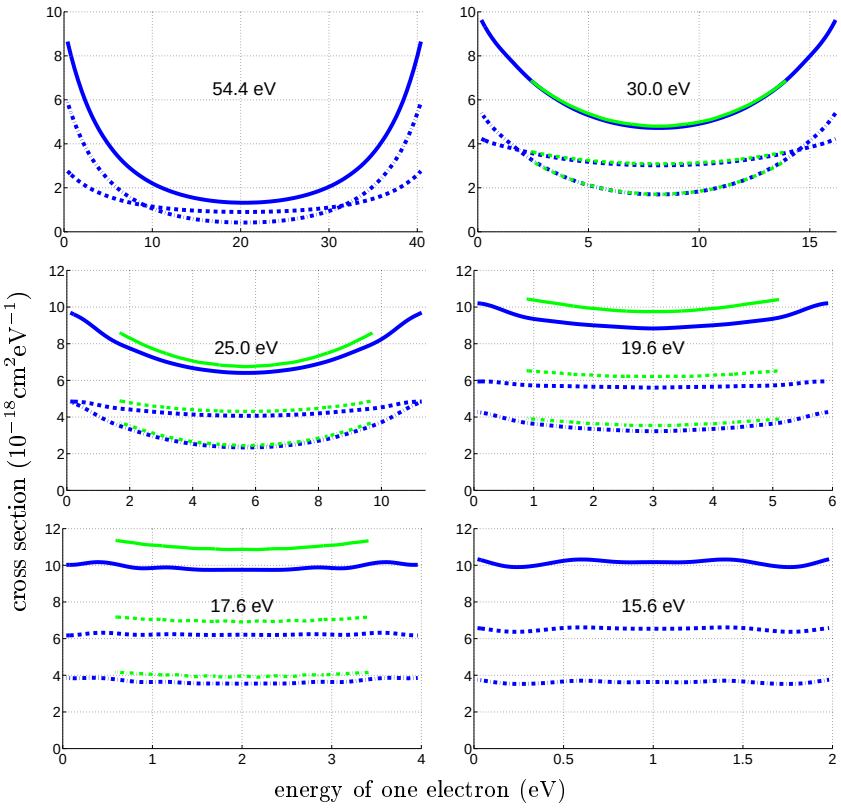

Fig. 5. Singly differential cross sections for e-H scattering at the collision energies indicated. Individual components for singlet (dashed line) and triplet (dot-dash line) are shown. Where applicable, results based on flux-extrapolation are shown in light gray.

the subtle departures from flatness as the SDCS turns from a "smile" at high energies to a nearly flat shape at energies near threshold.

5 Multi-Electron Targets

In electron-impact collisions involving more complicated atoms, even for a two-electron target, there are ionization processses that cannot occur for a one-electron atom: excitation-ionization, excitation-autoionization and double ionization. In excitation-ionization, the atom is singly ionized and the residual ion is left in an excited state. In excitation-autoionization, the target is first excited to an autoionizing state which can then decay into the ionization continuum in a process that competes with direct ionization at

the same energy. Double ionization is the (e,3e) process in which there are three free electrons in the final state.

While we are still far from the goal of carrying out a fully *ab initio* treatment of electron-impact ionization with a multi-electron target, there have already been a few proof-of-principle demonstrations involving model problems [33,26] that treat ionization of atomic targets with "two active electrons". These preliminary studies have served to establish the fact that time-dependent approaches certainly have the scaling properties that allow their application to three-electron systems and signal the emergence of a new level of sophistication in ionization studies that will go beyond currently available methods that treat multi-electron atoms with frozen-core, one-electron models.

5.1 Asymptotic Projection

The extraction of ionization cross sections from a numerical representation of the scattered wave on a finite grid is substantially more difficult with a multi-electron target than with a one-electron target. If one attempts to compute the ionization cross sections from an integral expression for the breakup amplitudes, one finds that in contrast to the one-electron target case, the use of distorted waves alone is not sufficient to eliminate numerical instabilities caused by discrete two-body channel terms in the scattered wave and additional steps are required to obtain a viable formula. To see why this is the case, we need only consider the asymptotic form of the scattered wave function for the case of a two-electron target at energies where both single ionization and two-body channels are open. For simplicity, we consider a case with no angular momentum. Asymptotically, there will be two-body terms in the scattered wave of the form $f_n e^{ik_n r_1}\chi_n(r_2,r_3)$, where $\chi_n(r_2,r_3)$ is a two-electron target bound state and f_n is the corresponding excitation amplitude, as well as an ionization term of the form $f^m_{ion}e^{ik\rho_{12}}\varphi_m(r_3)/\sqrt{\rho_{12}}$, where $\rho_{12}=\sqrt{r_1^2+r_2^2}$ and φ_m is a bound state of the residual ion.

Now suppose we attempt to compute the single ionization amplitude from an expression

$$f(k_1,k_2)=\int_S\Big(\phi_{k_1}(r_1)\phi_{k_2}(r_2)\varphi_n(r_3)\nabla\psi^+_{sc}(r_1,r_2,r_3)- \psi^+_{sc}(r_1,r_2,r_3)\nabla\phi_{k_1}(r_1)\phi_{k_2}(r_2)\varphi_n(r_3)\Big)\cdot\hat{\mathbf{n}}dS \tag{31}$$

which is an obvious generaliztion of Eq. (30) for a two-electron target. Since there is no orthogonality relation between the distorted waves and the *two-body* bound states, the two-body terms in the scattered wave will again give rise to overlaps between free functions in Eq. (31) which render it numerically unstable. One way to remedy this is to first evaluate the two-body amplitudes from the formula

$$f_n=2\langle sin(k_nr_1)\chi_n(r_2,r_3)|E-T-V_1|\Psi_{sc}\rangle, \tag{32}$$

since there are no formal or numerical problems associated with evaluation of Eq. (32). We can then construct an "asymptotically projected" scattered wave

$$\Psi_{sc}^{proj} = \Psi_{sc} - \sum_n (f_n/k_n) e^{ik_n r_1} \chi_n(r_2, r_3), \tag{33}$$

which removes the two-body channels from the asymptotic scattered wave. If we use Ψ_{sc}^{proj} in Eq. (31), then there is in principle no contamination of the ionization amplitude from two-body channels and the surface integral extracts the ionization amplitude just as it does in the case of a one-electron target.

When the collision energy moves above the threshold for double ionization, the asymptotic scattered wave will also contain a term proportional to $e^{iK\rho}/\rho$, where $\rho = \sqrt{r_1^2 + r_2^2 + r_3^2}$ and $E = K^2/2$. This term will again cause difficulties in the integral expression for the *single* ionization amplitude. Fortunately, the following integral can be used to compute the amplitude for double ionization:

$$f_{ion}^{double}(k_1, k_2, k_3) = \langle \phi_{k_1} \phi_{k_2} \phi_{k_3} | E - T - V_1 | \Psi_{sc}^{proj} \rangle, \tag{34}$$

where $E = k_1^2/2 + k_2^2/2 + k_3^2/2$. If the distorted waves are chosen to be eigenstates of the one-body potential, then orthogonality between the distorted waves and the one-body bound states φ_m prevents the asymptotic single-ionization terms in Ψ_{sc}^{proj} from causing any numerical problems. One can then extend the definition of Ψ_{sc}^{proj} to include the double ionization term,

$$\Psi_{sc}^{proj'} = \Psi_{sc} - \sum_n (f_n/k_n) e^{ik_n r_1} \chi_n(r_2, r_3) - f_{ion}^{double} e^{iK\rho}/\rho. \tag{35}$$

before using Eq. (31) to compute the amplitudes for single ionization. By following these steps, we can, in principle, compute all the scattering amplitudes of interest in the case of a two-electron target.

We have tested these ideas in a model 3-electron problem that involes only exponentially bound one- and two-body potentials [26]. The potential strengths were chosen so that the target 'atom' and 'ion' each bind a single state, so the only channels possible are elastic scattering and breakup. The scattered waves were computed on a three-dimensional radial grid by the time-dependent version of ECS outlined in Sec. 3.2. Fig. 6 plots the real part of the scattered wave for a fixed value of r_3, before and after projection of the elastic channel, at an incident energy of 11 eV. The elastic two-body component, clearly visible in the unprojected scattered wave near the r_1 and r_2 axes, are effectively removed by the asymptotic projection scheme adopted. In Table 1, we show the elastic scattering cross sections together with the total ionization cross sections computed by integrating the SDCS, the latter computed from the asymptotically projected scattered wave. The sum of these two quantities is the total cross section, which can be evaluated independently

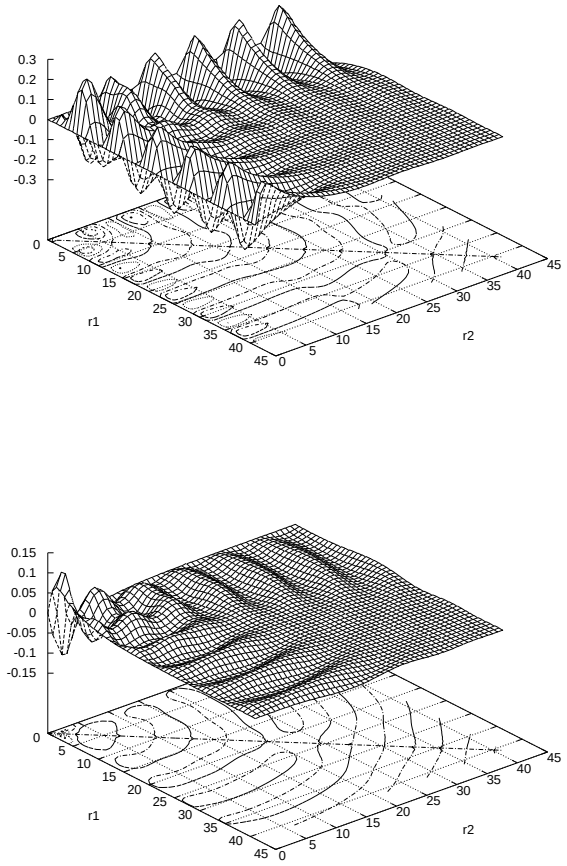

Fig. 6. Scattered wave, $\psi_{sc}^{(3)}$, for model 3D problem discussed in text, before (upper plot) and after (lower plot) asymptotic projection of elastic channel. All plotted quantities are in atomic units. The real part of $\psi_{sc}^{(3)}$ is plotted as a function of r_1 and r_2 with r_3 fixed at .1 bohr. The incident electron energy is 11 eV.

Table 1. Integrated cross sections for model 3D problem discussed in text.

$incidentenergy$	$\sigma_{elastic}$	σ_{ion}	$\sigma_{elastic}+\sigma_{ion}$	$\sigma_{optical}$	σ_{flux}
7 eV	17.238	3.173	20.411	19.681	20.237
9 eV	11.578	2.592	14.170	14.144	14.330
11 eV	8.568	2.176	10.744	10.708	10.883

from the optical theorem or from the total flux. The difference bedtween these quantities gives some indication of the overall numerical accuracy of the results.

6 Conclusion

Theoretical and computational advances over the past few years have brought us to a point where, for the simplest (e,2e) problems, it is accurate to say that the problem has been "reduced to practical computation". For such simple systems, it will shortly become a routine matter to computationally explore all aspects of collisional breakup, including noncoplanar geometries together with unequal energy sharing only a few volts above threshold. Dispite this progress, there are still questions to be answered, even in systems of only three charged particles. One notable problem yet to be solved is that of positron impact ionization where ionization competes with positronium formation. For collisional ionization of multi-electron atoms, there are still many details to be worked out and there are still open questions about what will ultimately prove to be the best way to extract ionization cross sections from the wave functions once they are available. Despite the challenges that remain, we are confident that benchmark calculations on the electron-helium system, similar to those that now exist for the electron-hydrogen system, will appear in the next few years.

Acknowledgments

This work was performed under the auspices of the U.S. Department of Energy by the University of California Lawrence Berkeley National Laboratory and Lawrence Livermore National Laboratory under contract numbers DE-AC03-76F00098 and W-7405-Eng-48, respectively. The work was supported by the US DOE Office of Basic Energy Science, Division of Chemical Sciences, and computations were performed on the computers of the National Energy Research Scientific Computing Center.

References

1. R. K. Peterkop, Opt. Spectrosc. **13**, 87 (1962).
2. M. R. H. Rudge and M. J. Seaton, Proc. Roy. Soc. A **283**, 262 (1965).
3. C. W. McCurdy, T. N. Rescigno, and D. Byrum, Phys. Rev. A **56**, 1958 (1997).
4. C. W. McCurdy and T. N. Rescigno, Phys. Rev. A **56**, R4369 (1997).
5. T. N. Rescigno, M. Baertschy, W. A. Isaacs, and C. W. McCurdy, Science **286**, 2474 (1999).
6. M. Baertschy, T. N. Rescigno, W. A. Isaacs, X. Li, and C. W. McCurdy, Phys. Rev. A **63**, 022712 (2000).

7. W. A. Isaacs, M. Baertschy, C. W. McCurdy, and T. N. Rescigno, Phys. Rev. A **63**, 030704R (2001).
8. M. Baertschy, T. N. Rescigno, and C. W. McCurdy, Phys. Rev. A **64**, 0022709 (2001).
9. I. Bray and A. T. Stelbovics, Phys. Rev. Letts. **69**, 53 (1992).
10. I. Bray, Phys. Rev. Letts. **78**, 4721 (1997).
11. I. Bray, J. Phys. B **33**, 581 (2000).
12. K. Bartschat and I. Bray, J. Phys. B **29**, L577 (1996).
13. D. Kato and S. Watanabe, Phys. Rev. Lett. **74**, 2443 (1995).
14. N. Miyashita, D. Kato, and S. Watanabe, Phys. Rev. A **59**, 4385 (1999).
15. M. S. Pindzola and F. Robicheaux, Phys. Rev. A **54**, 2142 (1996).
16. P. Selles, L. Malegat, and A. K. Kazansky, Phys. Rev. A **65**, 032711 (2002).
17. M. R. H. Rudge, Rev. Mod. Phys. **40**, 564 (1968).
18. B. Simon, Phys. Letts. A **71**, 211 (1979).
19. C. A. Nicolaides and D. R.Beck, Phys. Letts. A **65**, 11 (1978).
20. T. N. Rescigno, M. Baertschy, D. Byrum, and C. W. McCurdy, Phys. Rev. A **55**, 4253 (1997).
21. M. Baertschy, T. N. Rescigno, W. A. Isaacs, and C. W. McCurdy, Phys. Rev. A **60**(R13) (1999).
22. C. W. McCurdy and T. N. Rescigno, Phys. Rev. A **62**, 032712 (2000).
23. C. W. McCurdy, D. A. Horner, and T. N. Rescigno, Phys. Rev. A **63**, 022711 (2001).
24. J. W. Demmel, S. C. Eisenstat, J. R. Gilbert, X. S. Li, and J. W. H. Liu, SIAM J. Matrix Analysis and Applications **20**, 720 (1999).
25. T. N. Rescigno and C. W. McCurdy, Phys. Rev. A **62**, 032706 (2000).
26. C. W. McCurdy, D. A. Horner, and T. N. Rescigno, Phys. Rev. A **65**, 042714 (2002).
27. C. W. McCurdy and C. K. Stroud, Computer Phys. Comm. **63**, 323 (1991).
28. C. W. McCurdy, C. K. Stroud, and M. Wisinski, Phys. Rev. A **43**, 5980 (1991).
29. M. D. Feit, J. D. F. Jr., and A. Steiger, J. Comp. Phys. **47**, 412 (1982).
30. J. Röder, J. Rasch, K. Jung, C. T. Whelan, H. Ehrhardt, R. Allan, and H. Walters, *Phys. Rev. A* **53**, 225 (1996); J. Röder, H. Ehrhardt, C. Pan, A. F. Starace, I. Bray, and D. Fursa, *Phys. Rev. Lett.* **79**, 1666 (1997).
31. J. Röder, M. Baertschy, and I. Bray, Phys. Rev. A (2002), submitted.
32. J. M. Rost, Phys. Rev. Letts. **72**, 1998 (1994).
33. M. S. Pindzola, D. Mitnik, and F. Robicheaux, Phys. Rev. A **59**, 4390 (1999).